HOSTED BY

ELSEVIER

CrossMark

Available online at www.sciencedirect.com

ScienceDirect

Journal of Magnesium and Alloys 2 (2014) 220−224
www.elsevier.com/journals/journal-of-magnesium-and-alloys/2213-9567

Full length article

Influence of different extrusion processes on mechanical properties of magnesium alloy

Qingshan Yang [a,b,*], Bin Jiang [a,b,*], Hucheng Pan [c], Bo Song [d], Zhongtao Jiang [b], Jiahong Dai [b], Lifei Wang [b], Fusheng Pan [a,b]

[a] *Chongqing Academy of Science and Technology, Chongqing 401123, China*
[b] *National Engineering Research Center for Magnesium Alloys, Chongqing University, Chongqing 400044, China*
[c] *Key Laboratory for Anisotropy and Texture of Materials (Ministry of Education), Northeastern University, Shenyang 110004, Liaoning Province, China*
[d] *Faculty of Materials and Energy, Southwest University, Chongqing 400715, China*

Received 13 July 2014; revised 10 October 2014; accepted 10 October 2014
Available online 24 November 2014

Abstract

AZ31 Mg alloy sheets were processed by the conventional symmetrical extrusion (CSE) and the asymmetric extrusion (ASE). Progressive-asymmetric extrusion (PASE) and severe strain-asymmetric extrusion (SASE) were employed for ASE processes. The texture at near-surface and mid-layer zones of ASE sheets was diverse penetrating the normal direction (ND). This was attributed to an additional asymmetric shear strain deformation during the ASE process. (0002) basal planes of PASE sheets tilt to the shear deformation direction. Meanwhile, the basal texture intensity of PASE sheets has been weakened compared with one in CSE sheets. Grain refinement and tilted weak basal texture obtained by SASE process dramatically enhances the room temperature strength and plasticity of the extruded AZ31 magnesium alloy sheets. The microstructure and mechanical responses were examined and discussed.

Keywords: Mg alloys; Texture; Microstructure; Extrusion; Shear

1. Introduction

As lightest metallic materials, Mg alloy has been interest for the important advancement in the aerospace, automotive industries and tool applications [1−3]. Fabrications of the structural components principally concentrate upon tubes and sheets for these Mg alloys. Generally speaking, the dominant slip system of Mg alloy is the slip in the close packed direction $<11\bar{2}0>$ or $<a>$ on the (0002) basal planes at room temperature [4,5]. Thus, the magnesium alloys sheet normally produces the forceful basal texture during the extrusion and rolling approach [6,7]. And this further restricts the ductility of Mg alloy sheets with respect to their hexagonal close packed (*HCP*) crystal structure at room temperature.

It is well-known that the extrusion is an economical and practical process to yield the sectional materials such as sheets and bars. This can be grown into the structural components for the wrought Mg alloys [8,9]. Nevertheless, conventionally symmetrical extruded (CSE) magnesium alloy sheets reveal the inferior plasticity because of the finite quantity of the valid plastic deformation modes at room temperature [10,11]. Besides, Mg sheets with strong (0002) basal texture usually process the prominent anisotropy, the tension-compression-asymmetry and so on [12,13]. The room temperature formability mainly relies on the effect of the primal (0002) basal texture of Mg alloy sheets. Therefore, ameliorating texture

* Corresponding authors. Tel./fax: +86 023 6730 8621.
E-mail addresses: cquyqs@163.com (Q. Yang), jiangbinrong@cqu.edu.cn (B. Jiang).
Peer review under responsibility of National Engineering Research Center for Magnesium Alloys of China, Chongqing University.

http://dx.doi.org/10.1016/j.jma.2014.10.001.

should be considered as a valid method to improve the plasticity during the primary processing for Mg alloy sheets.

Many technologies were applied to modify the basal texture of Mg alloy sheets during the severe plastic deformation (SPD). Some research methods have yet used a lot of cockamamie and repetitive processes and thus were not able to the fabrication of the Mg alloy thin sheet [14,15]. It was found that differential speed rolling (DSR) process has effectively enhanced the ductility of Mg alloy sheets [16,17]. During the DSR process, the velocity of the up and down rolls was so different, resulting in the additional asymmetric shear strain deformation throughout the direction of the sheet thickness. The basal texture can be weakened during the DSR process. This asymmetric extrusion process is recommended to bring in the extrusion step under the strain path in one pass. In our work, the novel designed extrusion process is determined to modify the strong texture-dependent mechanical responses of Mg alloy sheets.

2. Experimental procedures

Cylindrical cast ingots of AZ31 Mg alloys (Mg-3 Al-1 Zn, in wt.%) with 82 mm in diameter was homogenized at 703 K for 2 h. These Mg alloys was carried out by the conventional symmetrical extrusion (CSE), the progressive-asymmetric extrusion (PASE) and severe strain-asymmetric extrusion (SASE), respectively. These ingots were extruded to the sheets of 1 mm thickness and 56 mm width at 703 K. Meanwhile, the speed of all extrusion processes was 20 mm/s with the extrusion ratio of 101.

The microstructures and the crystal orientation of Mg alloy sheets in the different extrusion processes were investigated by electron backscattered diffraction (EBSD) obtained using FEI Nova 400 FEG-SEM. The Mg alloy sheets were prepared for EBSD tests by electropolishing at 20 V for ~ 150 s in the AC2 solution. The (0002) basal texture was preformed on X-ray Rigaku D/Max 2500. The texture and EBSD datas were measured at upper surface, mid-layer and lower surface of ASE sheets (ND-ED plane). Here, ED, TD and ND respectively signify the extrusion direction, the transverse direction and the normal direction.

Dog-bone tensile samples with gage dimensions of 12 mm in length, 6 mm in width and 1 mm in thickness were machined from the Mg alloy sheets. Room temperature tensile tests were using by CMT6305-300 kN at the angles of 0°, 45° and 90° between the tensile and the extrusion direction at the strain rate of 10^{-3} s^{-1}.

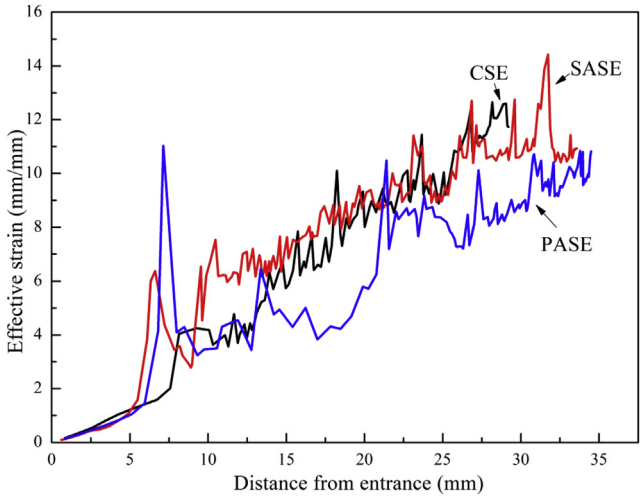

Fig. 2. The distribution of the effective strain of Mg alloy during the finite element models in the extrusion process.

3. Results and discussion

Fig. 1 reveals the schematic section of the flow passage in the conventional symmetrical extrusion (CSE), the progressive-asymmetric extrusion (PASE) and severe strain-asymmetric extrusion (SASE) dies, respectively. The velocity of the top and bottom surfaces during CSE process is the same because of a symmetric plane in the extrusion process. A great deal of the shear can be recommended through the space between the up and down surfaces along the parallel flow passage in the PASE and VASE dies equipped with a different length (L = 4 mm). Subsequently, this results in the asymmetric strain deformation in the normal direction of Mg alloy sheets in one pass extrusion during the ASE process.

The effective strain distribution of the Mg alloy sheet during the extrusion process was examined by the finite element model (FEM) in this work. For an easier comprehension of the extrusion process, the FEM results of CSE process were also analyzed to compare with those of ASE processes. Fig. 2 shows the effective strain of the workpiece processed by FEM during CSE, PASE and SASE processes, respectively. The waves in the effective strain curve are more uniform and stronger during the CSE process, while those of ASE express bigger ups and downs. In addition, it can be noted that the SASE process exhibits the highest value and PASE shows the lowest one. The effective strain curve shows the variation during the whole extrusion process for the AZ31

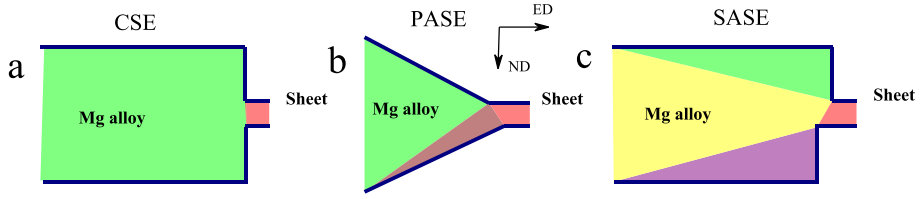

Fig. 1. Schematic section view of the extrusion die: (a) the conventional symmetrical extrusion (CSE), (b) the progressive-asymmetric extrusion (PASE) and (c) severe strain-asymmetric extrusion (SASE).

workpiece. Here, the peak denotes the maximum value of effective strain at this point. This signifies that SASE process would produce more asymmetric shear strain deformation.

Fig. 3 shows the (0002) basal texture and EBSD datas of the CSE, PASE and SASE samples in detail. The results were measured at up-surface, mid-layer and down -surface of ASE sheets. Microstructure of CSE samples were homogeneous with equiaxed dynamically recrystallized (DRX) grains of about 12 μm. Meanwhile, it can be seen that the CSE sheets generate the strong basal texture. The crystal orientation and basal texture of ASE sheets show totally various in the normal direction. Fig. 3(b) shows the microstructure at top surface of the PASE sheets was inhomogeneous with finer DRX grains. These grains were around a comparatively great area of elongated ones. Meanwhile, the basal texture at top surface of PASE sheets has decreased and tilted approximately 12° toward the extrusion direction. It is found that a considerable grain refinement is accomplished by the SASE process. Grain refinement mechanism was dominatingly ascribed to the grain subdivision [18–20]. SASE deformation can accommodate the strong plastic strain. As mentioned earlier, the simulation results indicate that the effective strain of the SASE is higher. Therefore, the grains of SASE are finer under the present shear strain path. In addition, the shear deformation makes the basal plane rotated to the direction of imposed shear strain during the ASE process in one continuous pass [21,22].

Mechanical properties are examined at various angles of 0°, 45° and 90° for CSE, PASE and SASE sheets at room

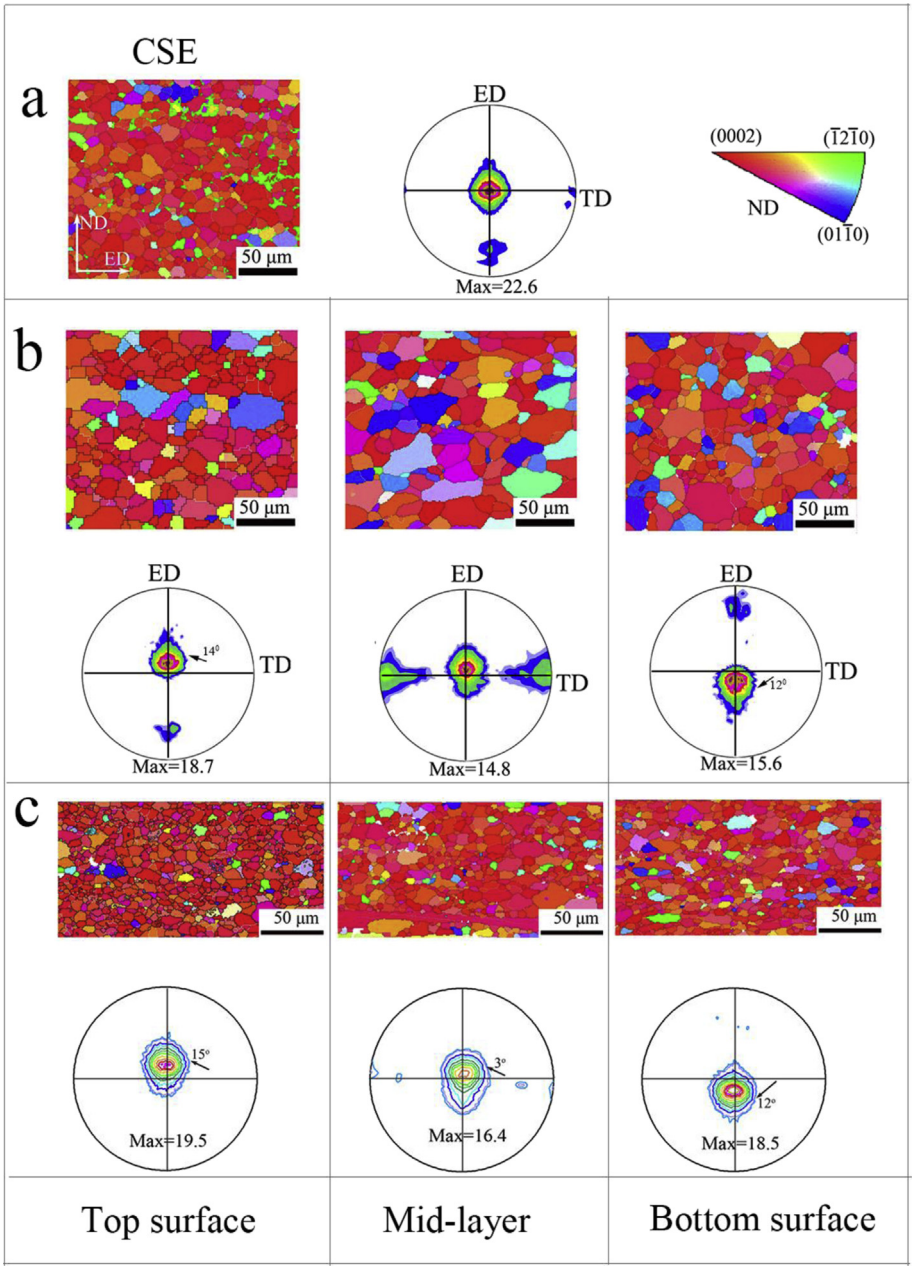

Fig. 3. (0002) Pole figures and EBSD orientation maps of the CSE (a), PASE (b) and (SASE) sheets.

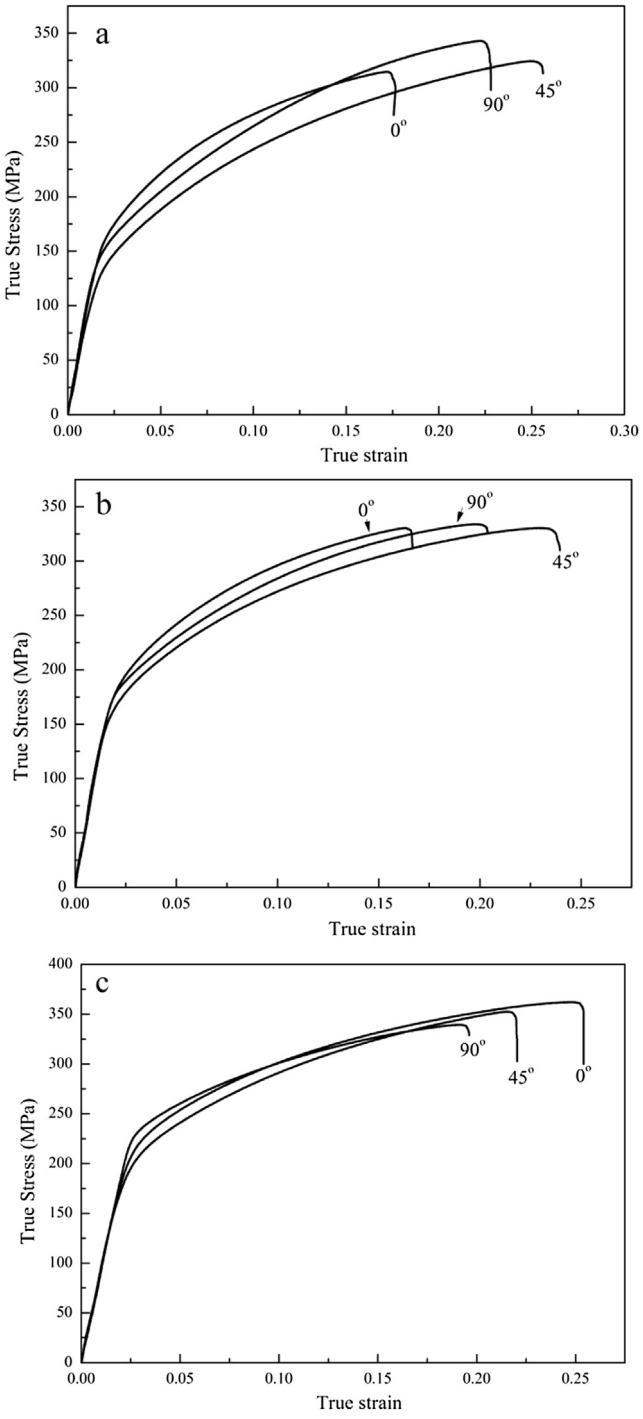

Fig. 4. True stress–strain curves during tensile tests in different directions (0°, 45° and 90°) of the CSE (a), PASE (b) and (SASE) sheets.

temperature, respectively. The true stress *vs*. true strain curves of these Mg alloy sheets are shown in Fig. 4. In general, based on (0002) basal planes of *HCP* crystal structure, the magnitude of macroscopic true stress (σ) and true plastic strain (ε) was referred to shear strain (γ) and resolved shear stress (τ). The corresponding relations among these parameters can be given by $\varepsilon = m_s\gamma$ and $\sigma = \tau/m_s$, where the parameter m_s is the Schmid factor of basal slip in Mg alloys. As seen from the stress–strain curves in Fig. 4, 45° samples have the highest E_u. It was because the Schmid factor (m_s), $m_s = \cos\lambda\cos\varphi$. Here, λ was the angle between the stress axis and the slip direction, and φ was the angle between the stress axis and the normal direction of slip plane. When $m_s = 0.5$ ($\lambda = 45°$, $\varphi = 45°$), it was near the maximum [23,24]. The values of mechanical properties such as yield stress (YS), the uniform elongation (E_u) and ultimate tensile strength (UTS) are summarized in Table 1. The average values of mechanical responses are given from the three different directions during the tensile tests. It can be expressed as $\overline{M} = (M_{0^\circ} + 2M_{45^\circ} + M_{90^\circ})/4$. It was found that there was a great difference in the mechanical performance of the extruded AZ31 Mg alloy sheets. The CSE sheets are not easy to deform during the plastic deformation because of the strong (0002) basal texture. The ASE sheets show superior ductility in every direction compared with those of the CSE sheets owing to the weak basal texture. The weaker texture intensity will result in a larger Schmid factor of <*a*> basal slip, which favors the improved ductility [20]. According to the Hall–Petch relation ($\sigma = \sigma_o + kd^{-1/2}$) [25,26], the strength of SASE sheets can be improved by the grain refinement. Furthermore, ASE process distinctly reduced mechanical anisotropy of AZ31 alloy sheets. The variation of the orientation factor in the basal slip of Mg alloys can affect the dislocation storage and the dynamic recovery. An additional shear in normal direction of sheets can accelerate non-basal slip systems during the ASE process. (0002) basal plane was rotated by the interactions of the multiple deformation model of Mg alloys [27,28]. The deformed microstructural structure should be needed to further make clear the deformation mechanism.

4. Conclusions

The mechanical properties of ASE sheets were outstandingly enhanced compared to those of CSE process. An additional shear in the ASE sheet thickness direction was developed, which lead to be more efficient in the plastic deformation. Meanwhile, the basal texture was weakened. This prompts the basal plane of PASE sheets to tilt

Table 1
Results of the tensile tests carried out in the tensile directions of 0°, 45° and 90°.

Sample	UTS (MPa)			YS (MPa)			E_u (%)			Average value		
	0°	45°	90°	0°	45°	90°	0°	45°	90°	UTS	YS	E_u
CE	332.0	322.8	331.0	161.2	147.7	168.6	15.4	22.1	19.0	327.2	156.3	19.7
PASE	315.4	326.4	344.3	149.5	124.7	135.7	16.4	23.7	22.1	328.1	133.7	21.5
SASE	352.8	364.3	341.5	179.9	198.3	225.0	20.1	22.8	18.7	355.7	200.4	21.1

approximately 12° to the extrusion direction. Moreover, FEM simulations show that SASE exhibits the highest values of the effective strain, which indicates that SASE process can be more effective in the grain refinement. Furthermore, the strength was notably enhanced in addition to reducing the yield asymmetry.

Acknowledgments

The authors are grateful for the financial supports from Chongqing Science and Technology Commission (CSTC2012JJJQ50001, CSTC2012GGB50003, CSTC2013 JCYJC60001), Youth Foundation of Chongqing academy of Science and Technology (2013CSTC-JBKY-00111), and National Natural Science Foundation of China (51171212 , 51474043).

References

[1] A.A. Luo, J. Magnesium Alloys 1 (2013) 2−22.
[2] G. Huang, L. Wang, H. Zhang, Y. Wang, Z. Shi, F. Pan, Mater. Lett. 98 (2013) 47−50.
[3] A. Chapuis, J.H. Driver, Acta Mater. 59 (2011) 1986−1994.
[4] A. Sankaran, S. Vadakke Madam, A. Nouri, M.R. Barnett, Scr. Mater. 66 (2012) 725−728.
[5] S. Xu, T. Liu, H. Chen, Z. Miao, Z. Zhang, W. Zeng, Mater. Sci. Eng. A 565 (2013) 96−101.
[6] R.L. Doiphode, S.V.S. Narayana Murty, N. Prabhu, B.P. Kashyap, J. Magnesium Alloys 1 (2013) 169−175.
[7] S.M. Arab, A. Akbarzadeh, J. Magnesium Alloys 1 (2013) 145−149.
[8] M.H. Maghsoudi, A. Zarei-Hanzaki, H.R. Abedi, Mater. Sci. Eng. A 595 (2014) 99−108.
[9] Q.S. Yang, B. Jiang, Y. Tian, W.J. Liu, F.S. Pan, Mater. Lett. 100 (2013) 29−31.
[10] J.-Y. Kang, B. Bacroix, R. Brenner, Scr. Mater. 66 (2012) 654−657.
[11] L.L. Chang, Y.N. Wang, X. Zhao, M. Qi, Mater. Charact. 60 (2009) 991−994.
[12] D.C. Foley, M. Al-Maharbi, K.T. Hartwig, I. Karaman, L.J. Kecskes, S.N. Mathaudhu, Scr. Mater. 64 (2011) 193−196.
[13] S. Yi, J. Bohlen, F. Heinemann, D. Letzig, Acta Mater. 58 (2010) 592−605.
[14] P. Mehrotra, T.M. Lillo, S.R. Agnew, Scr. Mater. 55 (2006) 855−858.
[15] X. Huang, K. Suzuki, N. Saito, Scr. Mater. 60 (2009) 651−654.
[16] L.L. Chang, S.B. Kang, J.H. Cho, Mater. Des. 44 (2013) 144−148.
[17] J. Suharto, Y.G. Ko, Mater. Sci. Eng. A 558 (2012) 90−94.
[18] Q. Yang, B. Jiang, J. He, B. Song, W. Liu, H. Dong, F. Pan, Mater. Sci. Eng. A 612 (2014) 187−191.
[19] H. Zhang, W. Jin, J. Fan, W. Cheng, H. Roven, B. Xu, H. Dong, Mater. Lett. 135 (2014) 31−34.
[20] H. Zhang, G. Huang, J. Fan, H. Roven, B. Xu, H. Dong, J. Alloys Compd. 615 (2014) 302−310.
[21] Loorentz, Y.G. Ko, J. Alloys Compd. 536 (2012) S122−S125.
[22] H. Zhang, G. Huang, J. Fan, H. Jørgen Roven, F. Pan, B. Xu, Mater. Sci. Eng. A 608 (2014) 234−241.
[23] J.A. del Valle, F. Carreño, O.A. Ruano, Acta Mater. 54 (2006) 4247−4259.
[24] S.M. Razavi, D.C. Foley, I. Karaman, K.T. Hartwig, O. Duygulu, L.J. Kecskes, S.N. Mathaudhu, V.H. Hammond, Scr. Mater. 67 (2012) 439−442.
[25] B. Song, R. Xin, G. Chen, X. Zhang, Q. Liu, Scr. Mater. 66 (2012) 1061−1064.
[26] N. Stanford, J. Geng, Y.B. Chun, C.H.J. Davies, J.F. Nie, M.R. Barnett, Acta Mater. 60 (2012) 218−228.
[27] Q.S. Yang, B. Jiang, G.Y. Zhou, J.H. Dai, F.S. Pan, Mater. Sci. Eng. A 590 (2014) 440−447.
[28] B. Hutchinson, J. Jain, M.R. Barnett, Acta Mater. 60 (2012) 5391−5398.